THE JOURNAL OF BIOLOGICAL CHEMISTRY VOL. 286, NO. 27, pp. 24253–24263, July 8, 2011

Identification of Novel Interaction Sites that Determine Specificity between Fibroblast Growth Factor Homologous Factors and Voltage-gated Sodium Channels*[S]

Received for publication, March 31, 2011, and in revised form, May 4, 2011 Published, JBC Papers in Press, May 12, 2011, DOI 10.1074/jbc.M111.245803

Chaojian Wang[1], **Chuan Wang**[1], **Ethan G. Hoch, and Geoffrey S. Pitt**[2]

From the Ion Channel Research Unit, Department of Medicine, Duke University Medical Center, Durham, North Carolina 27710

Fibroblast growth factor homologous factors (FHFs, FGF11–14) bind to the C termini (CTs) of specific voltage-gated sodium channels (VGSC) and thereby regulate their function. The effect of an individual FHF on a specific VGSC varies greatly depending upon the individual FHF isoform. How individual FHFs impart distinctive effects on specific VGSCs is not known and the specificity of these pairwise interactions is not understood. Using several biochemical approaches combined with functional analysis, we mapped the interaction site for FGF12B on the $Na_V1.5$ C terminus and discovered previously unknown determinants necessary for FGF12 interaction. Also, we demonstrated that FGF12B binds to some, but not all Na_V1 CTs, suggesting specificity of interaction. Exploiting a human single nucleotide polymorphism in the core domain of FGF12 (P149Q), we identified a surface proline that contributes a part of this pairwise specificity. This proline is conserved among all FHFs, and mutation of the homologous residue in FGF13 also leads to loss of interaction with a specific VGSC CT ($Na_V1.1$) and loss of modulation of the resultant Na^+ channel function. We hypothesized that some of the specificity mediated by this proline may result from differences in the affinity of the binding partners. Consistent with this hypothesis, surface plasmon resonance data showed that the P149Q mutation decreased the binding affinity between FHFs and VGSC CTs. Moreover, immunocytochemistry revealed that the mutation prevented proper subcellular targeting of FGF12 to the axon initial segment in neurons. Together, these results give new insights into details of the interactions between FHFs and $Na_V1.x$ CTs, and the consequent regulation of Na^+ channels.

The four fibroblast growth factor homologous factors, (FHFs,[3] FGF11–FGF14), are a distinct subset of the fibroblast growth factor (FGF) family. Lacking signal sequences, FHFs are not secreted. Moreover, although FHFs have FGF-like core domains, they contain specific deviations that render them unable to bind or activate FGF receptors; therefore they do not function as growth factors (1). Their function was unknown until a series of discoveries showed that FHFs are binding partners for the C termini (CTs) of certain voltage-gated sodium channels (VGSCs) and that FHFs can modulate Na^+ channel function (2, 3). Identification of the FGF14 gene as the locus for spinocerebellar ataxia 27 (SCA27) and the demonstration that the mutant form of FGF14 reduced Na^+ channel current and decreased neuronal excitability in a dominant negative manner (4, 5) underscored the physiological significance of FHFs as Na^+ channel modulators. Consistent with this role, FHFs are concentrated at the axon initial segment (AIS) and the nodes of Ranvier in neurons, the major locations where VGSCs reside (6, 7).

How FHFs bind to and modulate Na^+ channels remains uncertain. Each of the four FHFs has alternatively spliced N termini (NTs) preceding the FGF-like core (Fig. 1) and distinct NTs can confer differential Na^+ channel modulation (7, 8). Whether the alternatively spliced N termini interact directly with Na^+ channels to exert their specific effects is not known. Additionally, distinct FHFs have been shown to bind to specific $Na_V1.x$ C termini, suggesting a conserved region within the FHFs as the interaction site for $Na_V1.x$ CTs. Based on an observed dimerization of the FGF13 core within the asymmetric crystallographic unit, the dimer interface has been proposed as a binding surface for the $Na_V1.x$ CTs (9). Supporting data included the demonstration that mutation of residues on this interface's surface decreased affinity for various $Na_V1.x$ CTs, as measured by surface plasmon resonance (SPR) or by co-migration on a gel filtration column, and affected targeting of FGF13 to the AIS, although a surprising total of 8 simultaneous mutations was required for the full effects (9). On the Na^+ channel side of the interaction, the initial mapping of the FHF binding site placed it within the proximal portion of the intracellular VGSC CT (2, 3). This is surprising, since the structure of this region is highly conserved among VGSCs (10, 11) as shown in Fig. 1, yet specific FHFs interact with some $Na_V1.x$ CTs, but not with others. The restricted sets of pairwise interactions and consequent channel regulation are therefore intriguing observations. Understanding the underlying code is important for a full appreciation of FHF functions. We therefore set out to determine sources of the pairwise specificity by further defining the interaction sites between FHFs and $Na_V1.x$ CTs. We focused part of our attention on a nonsynonymous single nucleotide polymorphism (SNP) in the core domain of human FGF12B and wondered whether this SNP altered interaction

* This work was supported, in whole or in part, by Grants HL71165 and HL088089 from the National Institutes of Health and a Duke University SOM SR Voucher Program Award.

[S] The on-line version of this article (available at http://www.jbc.org) contains supplemental Fig. S1.

[1] Both authors participated equally in this work.

[2] An American Heart Association Established Investigator. To whom correspondence should be addressed: Box 103030 Med Center, Duke University, Durham, NC 27710. E-mail: geoffrey.pitt@duke.edu.

[3] The abbreviations used are: FHF, fibroblast growth factor homologous factor; AIS, axon initial segment; AnkG, ankyrin G; CaM, calmodulin; CT, C terminus; LQTS, Long QT Syndrome; SPR, surface plasmon resonance.

with Na^+ channels and consequent modulation of Na^+ currents. Using recombinant proteins we discovered new interaction determinants, which we validated functionally. These findings provide novel means with which to understand how FHFs bind to and modulate VGSCs.

EXPERIMENTAL PROCEDURES

Molecular Biology—Human clones were used as templates for all constructs. The following C-terminal fragments were cloned into pET28 (Novagen) which contains a sequence for a N-terminal His_6 tag: $Na_V1.1$ (amino acids 1789–1948; $Na_V1.1^{CT}$), $Na_V1.2$ (amino acids 1786–1922; $Na_V1.2^{CT}$), $Na_V1.5$ (amino acids 1773–1940; $Na_V1.5^{CT}$), $Na_V1.5$ (amino acids 1773–1887), $Na_V1.5$ (amino acids 1773–1908), $Na_V1.6$ (amino acid 1769–1926; $Na_V1.6^{CT}$), FGF12B (amino acids 1–181), and FGF13U (amino acids 1–192). FGF12B was also cloned into pMAL-c4G to obtain a maltose-binding protein (MBP) fusion protein. Additionally, $Na_V1.5$ (amino acids 1886–1908) was cloned into pGEX4T-1 (GE Healthcare). The following FHFs were cloned into pETDuet-1 (Invitrogen) in the second multiple cloning site, which does not contain a tag: FGF12B (amino acids 1–181), FGF13U (amino acids 1–192), and FGF13Y (amino acids 1–226). The FGF12B P149Q variant ($FGF12B^{P/Q}$; resulting from the single nucleotide polymorphism rs17852067) was obtained from American Type Culture Collection. The FGF13U P154Q mutant, and the $Na_V1.5$ truncation after amino acid 1885 (Δ1885) were generated by site-directed mutagenesis (QuikChange, Stratagene). For electrophysiology and co-immunoprecipitation, FGF12B, FGF13U, and FGF13U P154Q were cloned into pIRES2-acGFP1 (Clontech) with the His_6 tag at the C terminus. A HEK cell line stably expressing $Na_V1.1$ was obtained from Alfred George (Vanderbilt University). An expression construct for $Na_V1.2$ was obtained from Theodore Cummins (Indiana University). An expression construct for $Na_V1.5$ was obtained from Nenad Bursac (Duke University). For expression in hippocampal neurons, FGF12B and $FGF12B^{P/Q}$ were cloned into pEGFP-N3 (Clontech). All constructions and mutations were verified by DNA sequence analysis.

Recombinant Protein Expression and Co-purification—Proteins were expressed in BL-21 (DE3) cells after induction with 1 mM isopropyl-1-thio-β-D-galactopyranoside (IPTG) for 64 h at 16 °C. Cells were harvested and resuspended in 300 mM NaCl, 20 mM Tris-HCl, 5 mM imidazole, pH 7.5, supplemented with EDTA-free protease inhibitor mixture (Roche). Cell extracts were prepared by passage twice through an Avestin homogenizer (Emulsiflex-C5, Canada) then centrifuged at 100,000 × *g* for 25 min. The purification protocol has been previously described (12). In the absence of an expressed His_6 tag protein nothing purified by metal affinity chromatography. In some cases, faint nonspecific bands, at sub-stoichiometric ratios, are visible after purification. The proteins used for surface plasmon resonance analysis were further purified by gel filtration on a Superdex 75 10/300L column on an AKTA FPLC (GE Healthcare) in 300 mM NaCl, 20 mM Tris-HCl, pH 7.5 with 1 mM DTT. Supernatants of GST-tagged protein complexes were applied to glutathione-Sepharose 4B (GE Healthcare). The column was then washed with buffer containing 300 mM NaCl, 20 mM Tris-HCl, pH 7.5, and proteins were eluted in above buffer supplemented with 10 mM glutathione, pH 7.5. Supernatants of MBP-tagged protein complexes were applied to amylose resin (New England Biolab) in a buffer containing 300 mM NaCl, 20 mM Tris-HCl pH 7.5, 1 mM EDTA. The column was washed extensively with the same buffer, and proteins were then eluted in the same buffer supplemented with 10 mM maltose, pH 7.5. Each experiment was repeated at least three independent times, and the gels are representative of all experiments.

Protein Expression and co-IP in HEK Cells—HEK293T cells or $Na_V1.1$ stable cell lines were transfected at ~80% confluence using Lipofectamine 2000 (Invitrogen). For HEK293T cells, the total amount of DNA for 60-mm plates was 8 μg. For the $Na_V1.1$ stable cell line 2 μg of FGF13U or $FGF13U^{P/Q}$ was transfected for a 60-mm plate. 2 μg of the empty pIRES2-acGFP1 vector was used as a negative control. Transfected cells were washed with ice-cold PBS 24 h after transfection, and cell lysates were prepared with the addition of lysis buffer containing 150 mM NaCl, 50 mM Tris-HCl, pH 7.5, 1% Triton with protease inhibitor mixture (Roche). The pelleted cells were pipetted up and down 20 times with lysis buffer and then passed 20 times through a 22 gauge needle, incubated at 4 °C for 1 h and then centrifuged at 16,000 × *g* for 10 min at 4 °C. The lysates were precleared by exposure to 20 μl of protein A/G-agarose beads (Santa Cruz Biotechnology) for 30 min at 4 °C. The protein concentration was determined using the BCA Protein Assay kit. Immunoprecipitation was performed with 1 μg of anti-His_6 (Qiagen) antibody added to 100 μg of precleared lysates. The samples were rocked gently at 4 °C for 1 h followed by addition of 30 μl of protein A/G-agarose slurry. The samples were rotated overnight at 4 °C and centrifuged at 7000 rpm for 2 min. After washing with lysis buffer three times, 40 μl of loading buffer was added to the pellet, and protein was eluted from the beads by heating at 70 °C for 20 min. The samples were subjected to NuPAGE 8–16% Bis-Tris gels (Invitrogen). As a negative control, parallel reactions were performed with mouse IgG. The proteins were transferred to nitrocellulose membranes and subsequently immunoblotted with the anti-His antibody or an anti-pan Na_V antibody (Sigma). The blots were visualized by enhanced chemiluminescence, and images were captured with a Kodak Image Station 4000 R.

Analysis of FHF Channel Interactions by Surface Plasmon Resonance Spectroscopy (SPR)—SPR experiments were performed on a Biacore 3000 instrument (Biacore AB) in the Duke University Biomolecular Interaction Analysis Core Facility. The interactions between FHF-Nav1.x pairs were studied at 25 °C. To analyze FHF binding to the $Na_V1.x$ C-terminal domains, the following were immobilized by amine coupling on three flow channels of CM5 chip: FGF12B (18.27 fmol/mm^2), $FGF12B^{P/Q}$ (24.02 fmol/mm^2), and FGF13 (21 fmol/mm^2). Bovine serum albumin (8 fmol/mm) was coupled to the control flow channel of the chip for nonspecific binding. Increasing concentrations (25 μg/μl-100 μg/μl) of the $Na_V1.x$ CTs in Tris-HCl buffer (20 mm Tris-HCl, pH 7.5, 300 mm NaCl, 1 mM DTT) were injected over the chip at a flow rate of 50 μl min^{-1}. At the end of each protein injection (300 s), Tris-HCl buffer at 50 μl min^{-1} was flowed over the chip for 300 s to monitor dissociation. The chip surface was then regenerated by inject-

ing 50 μl of 2.0 M NaCl in 10 mM sodium acetate, pH 4.5 at a flow rate 50 μl min^{-1}. The data were processed with BiaEvaluation 4.1 software (Biacore AB). For each $Na_V1.x$ injection, the nonspecific responses from the BSA control flow channel were subtracted from the responses recorded for each FHF flow channel. Because data analysis revealed no signal from the $FGF12B^{P/Q}$ -$Na_V1.1$ interaction, this was then used for subtraction of nonspecific responses. The specific binding responses were fitted globally using a 1:1 Langmuir binding model to estimate equilibrium dissociation constants.

Electrophysiology—HEK293 cells were transfected at 80–90% confluence using Lipofectamine 2000 (Invitrogen) according to the manufacturer's instructions. The total amount of DNA for all transfections was kept constant. Transfected cells were identified by GFP fluorescence. Na^+ currents were recorded using the whole-cell patch-clamp technique at room temperature (20–22 °C) 48–72 h after transfection. Electrode resistance ranged from 1–2 MΩ. Currents were filtered at 5 kHz and digitized using an analog-to-digital interface (Digidata 1322A, Axon Instruments). Capacitance and series resistance were adjusted (70–85%) to obtain minimal contribution of the capacitive transients. The bath solution contained (in mM): NaCl 130, KCl 4, $CaCl_2$ 1.8, $MgCl_2$ 1, HEPES 10, glucose 10, pH 7.35 (adjusted with NaOH). The intracellular solution contained (in mM): CsF 110, EGTA 10, NaF 10, CsCl 20, HEPES 10, pH 7.35 (adjusted with CsOH). Osmolarity was adjusted to 310 mOsm with sucrose for all solutions. Standard two-pulse protocols were used to generate the steady-state inactivation curves: from a holding potential of −120 mV, cells were stepped to 500-ms preconditioning potentials varying between −130 mV and −10 mV (prepulse), followed by a 20 ms test pulse to −20 mV. Currents (I) were normalized to I_{max} and fit to a Boltzmann function of the form $I/I_{max} = 1/\{1+\exp[(V_m - V_{1/2})/k]\}$ in which $V_{1/2}$ is the voltage at which half of Nav1.5 channels are inactivated, k is the slope factor and V_m is the membrane potential. Data analysis was performed using Clampfit 10.2 software (Axon Instruments) and Origin 8 (Originlab Corporation). Results are presented as means ± S.E.; the statistical significance of differences between groups was assessed using a two-tailed Student's t test and was set at $p < 0.05$.

Neuronal Cultures—Animal studies were approved by the Institutional Animal Care and Use Committee of Duke University and conformed to the Guide for the Care and Use of Laboratory Animals published by the United States National Institutes of Health (NIH Publication No. 85-23, revised 1996). Hippocampi from embryonic day 18 rats (Sprague-Dawley) were dissociated through enzymatic treatment with 0.25% trypsin and subsequent trituration. The neurons were plated on glass coverslips previously coated with poly-D-lysine. Neurons were grown in neurobasal A medium (Invitrogen, Carlsbad, CA) supplemented with 2% B27, 2 mM glutamine, and 10% heat-inactivated bovine calf serum. After 24 h, this medium was replaced by media containing 0.5 mM glutamine, 1% heat-inactivated bovine calf serum, 0.5 mM kynurenic acid, 70 μM uridine, and 25 μM 5-fluorodeoxyuridine. Hippocampal neurons grown for 6–7 days in culture were transfected with GFP-FGF12B or GFP-$FGF12B^{P/Q}$ using Lipofectamine 2000 (Invitrogen).

Immunofluorescence and Imaging—Hippocampal neurons (2 days after transfection) were fixed in fresh 4% paraformaldehyde in PBS for 5 min and permeabilized with 0.1% Triton X-100. After blocking with 10% goat serum for 30 min at 37 °C, neurons were incubated at 4 °C for 12–16 h with a monoclonal ankyrin G antibody (1:1000, a gift from Van Bennett, Duke University) diluted in PBS containing 10% goat serum. Neurons were then washed three times in PBS and incubated for 1 h at 37 °C with Cy3 goat anti-mouse IgG (1:1000, Jackson Immunoresearch). After three washes with PBS, coverslips were mounted in Citifluor mounting media (Ted Pella Inc.). Images were acquired using a Bio-Rad MRC 1000 confocal laser scanning system coupled to a Zeiss Axiovert 100 inverted microscope and scored by an observer blinded to the identity of the co-transfected FHF. Statistical comparison was done by χ^2 analysis.

RESULTS

Mapping the FGF12B Interaction Site within the $Na_V1.5^{CT}$—A working model for FHF interactions with $Na_V1.x$ C termini posits that a conserved domain within the FGF-like core binds to a domain within the proximal portion of a $Na_V1.x$ C terminus, a region highly conserved among VGSCs (9). However, this model cannot explain the FHF isoform specificity observed for interaction with, and modulation of, VSGCs (3, 7). Because mapping of the FHF binding site within $Na_V1.x$ CTs initially utilized a yeast two-hybrid approach that cannot rule out an interaction mediated by another binding partner expressed in yeast and is also an indirect assessment of binding (read-out is viability and/or gene reporter activation), we tested for a direct interaction between purified, recombinant proteins to determine the FGF12B binding site on the $Na_V1.5^{CT}$. We chose FGF12B (FHF1B) since it showed significant specificity in binding among multiple $Na_V1.x$ CTs in the yeast two-hybrid experiments, and we chose $Na_V1.5^{CT}$ because it appeared to show a strong interaction with FGF12B (3). We co-expressed FGF12B in *Escherichia coli* along with a His_6-tagged $Na_V1.5$ CT and tested whether un-tagged FGF12B co-purified along with the $Na_V1.5$ CT during purification by metal affinity chromatography. Our starting $Na_V1.5$ CT construct was an extended domain from the end of IVS6 (amino acid 1773) to amino acid 1940, which includes proximal regions highly conserved among all Na_V1 CT domains and regions more distal that are less conserved (Figs. 1 and 2*A*). Co-expression of the His_6-tagged $Na_V1.5^{CT}$ (amino acids 1773–1940) with un-tagged FGF12B followed by purification by metal affinity chromatography resulted in efficient and stoichiometric co-purification of FGF12B as detected by Coomassie Blue staining (Fig. 2*B*). The absence of other bacterial proteins observed in the gel demonstrates that the binding between the $Na_V1.5^{CT}$ and FGF12B was direct. Thus, our co-purification approach offers a means to assess direct interactions between a $Na_V1.x$ and a FHF.

To attempt to define specific binding determinants within the $Na_V1.5$ CT, we then generated a shorter construct by deleting from the C terminus to amino acid 1908. This truncation also bound FGF12B, as shown in Fig. 2*B*. These results are consistent with the interaction observed with a $Na_V1.5^{CT}$ containing amino acids 1773–1911 (9). We further deleted the

A

```
FGF12A      1    MAAAIASSLI RQKR--QARE S--NSDRVSA SKRRSSPSKD GRSLCERHVL GVFS----KV RFCSGRKRPV RRRPEPQLKG
FGF12B      1    ---------- ---------- ---------- ---------- ---------- ----------M ESK------- ----EPQLKG
FGF13S      1    MAAAIASSLI RQKR-QARER EKSNACKCVS SPSKGKTSCD KNKLNVFSRV KLFG------ ---SKKRR-- RRRPEPQLKG
FGF13U      1    ---------- ---------- ---------- -------MAL LRK------- ---------- ---------- -SYSEPQLKG
FGF13V      1    ---------- ---------- ---------- ------MSGK VTK-P----- ---------- -K---EEK-- DASKEPQLKG
FGF13Y      1    ---------- ---------- ---------M LRQDSIQSAE LKKKESPFRA KCHEIFCCPL KQVHHKEN-- TEPEEPQLKG
FGF13YV     1    MSGKVTKPKE EKDASKVLDD APPGTQEYIM LRQDSIQSAE LKKKESPFRA KCHEIFCCPL KQVHHKEN-- TEPEEPQLKG

FGF12A     73    IVTRLFSQQG YFLQMHPDGT IDGTKDENSD YTLFNLIPVG LRVVAIQGVK ASLYVAMNGE GYLYSSDVFT PECKFKESVF
FGF12B     11    IVTRLFSQQG YFLQMHPDGT IDGTKDENSD YTLFNLIPVG LRVVAIQGVK ASLYVAMNGE GYLYSSDVFT PECKFKESVF
FGF13S     69    IVTKLYSRQG YHLQLQADGT IDGTKDEDST YTLFNLIPVG LRVVAIQGVQ TKLYLAMNSE GYLYTSELFT PECKFKESVF
FGF13U     16    IVTKLYSRQG YHLQLQADGT IDGTKDEDST YTLFNLIPVG LRVVAIQGVQ TKLYLAMNSE GYLYTSELFT PECKFKESVF
FGF13V     23    IVTKLYSRQG YHLQLQADGT IDGTKDEDST YTLFNLIPVG LRVVAIQGVQ TKLYLAMNSE GYLYTSELFT PECKFKESVF
FGF13Y     50    IVTKLYSRQG YHLQLQADGT IDGTKDEDST YTLFNLIPVG LRVVAIQGVQ TKLYLAMNSE GYLYTSELFT PECKFKESVF
FGF13YV    79    IVTKLYSRQG YHLQLQADGT IDGTKDEDST YTLFNLIPVG LRVVAIQGVQ TKLYLAMNSE GYLYTSELFT PECKFKESVF

FGF12A    153    ENYYVIYSST LYRQQESGRA WFLGLNKEGQ IMKGNRVKKT KPSSHFVPKP IEVCMYREPS LHEIGEKQ-- --GRSRKS-S GTPTMNGGKV VNQ-DST
FGF12B     91    ENYYVIYSST LYRQQESGRA WFLGLNKEGQ IMKGNRVKKT KPSSHFVPKP IEVCMYREPS LHEIGEKQ-- --GRSRKS-S GTPTMNGGKV VNQ-DST
FGF13S    149    ENYYVTYSSM IYRQQQSGRG WYLGLNKEGE IMKGNHVKKN KPAAHFLPKP LKVAMYKEPS LHDLTEFSRS GSGTPTKSRS VSGVLNGGKS MSHNEST
FGHF2U     96    ENYYVTYSSM IYRQQQSGRG WYLGLNKEGE IMKGNHVKKN KPAAHFLPKP LKVAMYKEPS LHDLTEFSRS GSGTPTKSRS VSGVLNGGKS MSHNEST
FGF13V    103    ENYYVTYSSM IYRQQQSGRG WYLGLNKEGE IMKGNHVKKN KPAAHFLPKP LKVAMYKEPS LHDLTEFSRS GSGTPTKSRS VSGVLNGGKS MSHNEST
FGF13Y    130    ENYYVTYSSM IYRQQQSGRG WYLGLNKEGE IMKGNHVKKN KPAAHFLPKP LKVAMYKEPS LHDLTEFSRS GSGTPTKSRS VSGVLNGGKS MSHNEST
FGF13YV   159    ENYYVTYSSM IYRQQQSGRG WYLGLNKEGE IMKGNHVKKN KPAAHFLPKP LKVAMYKEPS LHDLTEFSRS GSGTPTKSRS VSGVLNGGKS MSHNEST
                                                                                  *
```

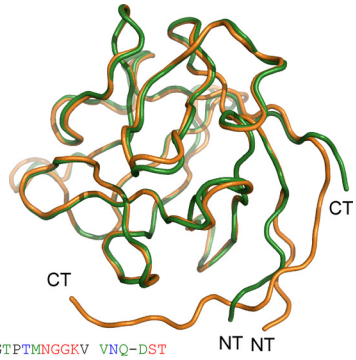

B

```
Na$_V$1.1   1787    ENFSVATEES AEPLSEDDFE MFYEVWEKFD PDATQFMEFE KLSQFAAALE PPLNLPQPNK LQLIAMDLPM VSGDRIHCLD ILFAFTKRVL
Na$_V$1.2   1777    ENFSVATEES AEPLSEDDFE MFYEVWEKFD PDATQFIEFA KLSDFADALD PPLLIAKPNK VQLIAMDLPM VSGDRIHCLD ILFAFTKRVL
Na$_V$1.5   1773    ENFSVATEES TEPLSEDDFD MFYEIWEKFD PEATQFIEYS VLSDFADALS EPLRIAKPNQ ISLINMDLPM VSGDRIHCMD ILFAFTKRVL
Na$_V$1.6   1767    ENFSVATEES ADPLSEDDFE TFYEIWEKFD PDATQFIEYC KLADFADALE HPLRVPKPNT IELIAMDLPM VSGDRIHCLD ILFAFTKRVL

Na$_V$1.1   1877    GESGEMDALR IQMEERFMAS NPSKVSYQPI TTTLKRKQEE VSAVIIQRAY RRHLLKRTVK QASFTYNKNK IKGG--ANLL IKEDMIIDRI
Na$_V$1.2   1867    GESGEMDALR IQMEERFMAS NPSKVSYEPI TTTLKRKQEE VSAIIIQRAY RRYLLKQKVK KVSSIYKKDK GKEC--DGTP IKEDTLIDKL
Na$_V$1.5   1863    GESGEMDALK IQMEEKFMAA NPSKISYEPI TTTLRRKHEE VSAMVIQRAF RRHLLQRSLK HASFLFRQQA GSGLSEEDAP EREGLIAYVM
Na$_V$1.6   1857    GDSGELDILR QQMEERFVAS NPSKVSYEPI TTTLRRKQEE VSAVVLQRAY RGHLARR--- -G-FICKKTT SN-------- KLE-------

Na$_V$1.1   1962    NENSITEKT- --DLTMSTAA CPPSYDRVTK PIVEKHE--- -----QEGKD EKAKG-K--- ----
Na$_V$1.2   1952    NENSTPEKT- --DMTPSTTS -PPSYDSVTK PEKEKFE--- -----KDKSE KEDKG-KDIR ESKK
Na$_V$1.5   1953    SENFSRPLGP PSSSSISSTS FPPSYDSVTR ATSDNLQVRG SDYSHSEDLA DFPPSPDRDR ESIV
Na$_V$1.6   1924    NGGTHREKK- --ESTPSTAS -LPSYDSVTK PEKEKQQRA- -----EEGRR ERAKRQKEVR ESKC
```

FIGURE 1. **The FGF12 and FGF13 core domains and the Na$_V$1 C termini are highly conserved.** Multiple sequence alignment using ClustalW of human FGF12 and FGF13 isoforms (*A*) and the human Na$_V$1.1, Na$_V$1.2, Na$_V$1.5, and Na$_V$1.6 C termini, beginning at the end of the predicted IVS6 transmembrane helix (*B*). *Red* indicates complete identity, *green* indicates strong similarity, *blue* indicates weak similarity, and *black* indicates difference. To the *right* of each alignment are ribbon structures for the core domains of FGF12 (*green*, PDB: 1Q1U) and FGF13 (*orange*, PDB: 3HBW) in *A*., and Na$_V$1.2 (*orange*, PDB: 2KAV) and Na$_V$1.5 (*green*, PDB: 2KBI) in B. *Gray shading* in the alignments indicates the portion of the sequences observed in the ribbon structures. The proline (Pro^{211} in FGF12A and Pro^{149} in FGF12B) affected by the SNP is indicated by * in *A*.

Na$_V$1.5^{CT} to amino acid 1887 (Fig. 2*B*), since the protein from amino acid 1773–1887 is a structurally well-defined domain within the most highly conserved region of the VGSC CTs and atomic structural information is also available (10, 11); it is therefore well-suited as a reagent for these types of binding experiments. In contrast to the previous yeast-two hybrid results with a shorter construct (amino acids 1773–1832), purification of the His$_6$-tagged Na$_V$1.5^{CT} construct containing amino acids 1773–1887 did not yield co-purification of FGF12B (Fig. 2*B*).

Because our results differed from the yeast-two hybrid mapping, we then confirmed our results using a co-immunoprecipitation strategy and functional validation by electrophysiology. As shown in Fig. 2*C*, full-length Na$_V$1.5 co-immunoprecipitated from a 16,000 × *g* lysate with a co-expressed His$_6$-tagged FGF12B, but a Na$_V$1.5 truncated after amino acid 1885 (Δ1885) did not. While a 16,000 × *g* lysate may contain elements of endoplasmic reticulum membranes (as compared with a 100,000 × *g* lysate), the distinct results obtained with full-length compared with Δ1885 channels demonstrates that the truncation abolished means of interaction with FGF12B.The Δ1885 construct was chosen because this truncation is able to yield a functional VGSC (15). We could therefore test whether the lack of interaction with FGF12B, as assessed by co-immunoprecipitation, correlated with an absence of functional modulation. Na^+ currents were recorded in HEK293 cells similarly transfected with Na$_V$1.5, or Δ1885, and FGF12B. Example current traces are shown in Fig. 2*D*. Current density was not affected by the truncation (180 ± 26 *versus* 187 ± 15 pA/pF for full-length *versus* Δ1885, $p > 0.05$). Current density was also not different between the full length channel and Δ1885 when FGF12B was co-expressed (135 ± 28 pA/pF *versus* 134 ± 30 pA/pF for full-length *versus* Δ1885, $p > 0.05$). However, current density in heterologous expression systems can be affected by multiple factors that are independent of the interaction between the channel and the FHF, such as biosynthesis, trafficking, and targeting of one of the added components. In contrast, channel gating (*e.g.* inactivation), regulated by the direct interaction of the expressed components, is a better measure for assessing the consequences of the interaction (or lack thereof) between Na$_V$1.5 and FGF12B, because any observed effect is less sensitive to differences in stoichiometry. For the full-length channel addition of FGF12B shifted the $V_{1/2}$ of steady-state inactivation by +6 mV (Fig. 2*E* and Table 1), demonstrating the modulatory effect of the FHF. Steady-state inactivation for the Δ1885 truncated channel was shifted −4 mV compared with the full-length channel, as previously reported (15), but the addition of FGF12B had no effect upon Δ1885. Thus, the lack of binding between purified, recombinant FGF12B and the Na$_V$1.5 CT truncated at amino acid 1887 (Fig.

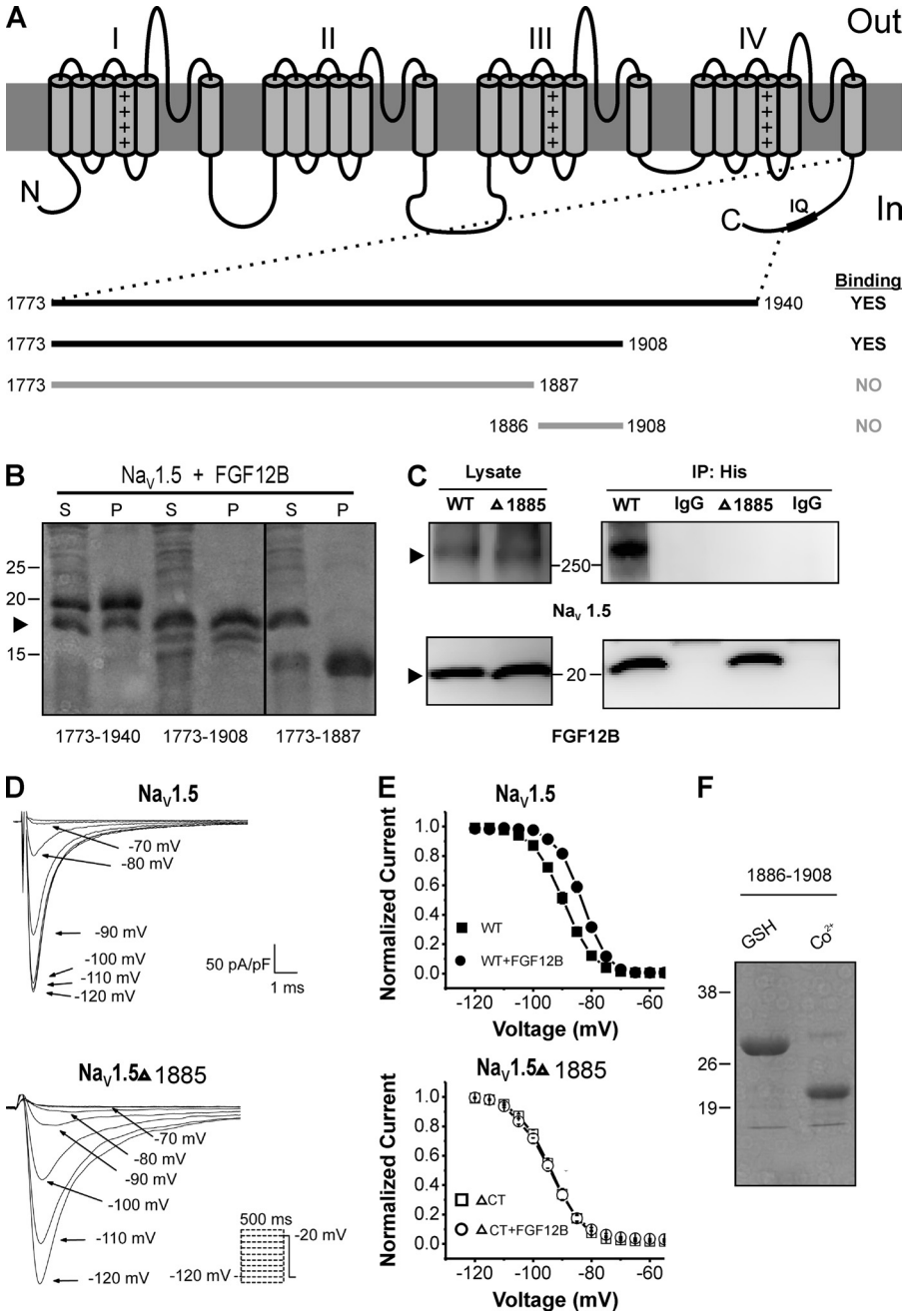

FIGURE 2. **Mapping the interaction site for FGF12B on Na$_V$1.5 CT.** *A*, schematic of the Na$_V$1.5 channel (the calmodulin binding IQ motif in the CT is indicated), the constructs used in mapping, and the overall mapping results for FGF12B binding. *B*, Coomassie-stained SDS-PAGE shows FGF12B co-purification with the indicated His$_6$-tagged Na$_V$1.5^{CT}. FGF12B co-purified with constructs containing sequences through amino acid 1908, but further truncation (to amino acid 1887) abolished binding. *S*, supernatant of bacterial cell lysate; *P*, metal-affinity purified protein. *C*, co-immunoprecipitation from HEK293 cell lysates of His$_6$-tagged FGF12B with Na$_V$1.5 or an Na$_V$1.5 truncated after amino acid 1885 (Δ1885). The truncated channel does not interact with FGF12B. *D*, example current traces for the full-length Na$_V$1.5 or Δ1885 used to calculate steady-state inactivation. Scale bars and the protocol used are shown as *insets*. *E*, steady-state inactivation data for Na$_V$1.5 and Δ1885, each with or without FGF12B. *Symbols* at each test potential show average ± S.E. *Lines* show fits to Boltzmann distributions (see "Experimental Procedures"); parameters, statistics, and *N* are in Table 1. *F*, lack of interaction between a GST-tagged Na$_V$1.5 CT construct (amino acids 1886–1908) and the His$_6$-tagged FGF12B.

2*B*) correlates with the absence of interaction between the Δ1885 channel and FGF12B, as assessed by co-immunoprecipitation and functional electrophysiology. Together, these data, suggest that at least some key determinants for FHF interaction lie outside of the proximal region of the Na$_V$1.5 CT previously implicated in binding (3). Moreover, these data demonstrate the utility of the recombinant protein assay to define binding determinants.

The different results obtained with the 1773–1887 and the 1773–1908 constructs suggested that the region between 1887 and 1908 may contain critical determinants for binding. We tested this directly by generating a GST-tagged protein containing amino acids 1886–1908 and assayed whether it was able to co-purify a co-expressed (in *E. coli*) His$_6$-tagged FGF12B. The resultant bacterial lysate was split; half was purified by glutathione-agarose and half by Co^{2+}-affinity resin. As seen in

TABLE 1
Steady state inactivation parameters for the indicated Na$_V$1.x channel with a specific FHF

	Na$_V$1.1			Na$_V$1.2			Na$_V$1.5			Na$_V$1.5 Δ1885		
	$V_{1/2}$	k	n	$V_{1/2}$	k	n	$V_{1/2}$	k	n	$V_{1/2}$	k	n
None	−54.1 ± 1.5	5.3 ± 0.3	8	−65.0 ± 1.3	4.7 ± 0.1	6	−89.8 ± 0.8	4.7 ± 0.1	14	−93.9 ± 0.8	5.2 ± 0.2	11
FGF12B	−55.1 ± 1.5	4.4 ± 0.1	6	−57.0 ± 1.6[a]	4.6 ± 0.4	5	−83.8 ± 0.7[a]	4.0 ± 0.1[a]	6	−94.7 ± 0.9	5.6 ± 0.1[a]	10
FGF12B$^{P/Q}$	−53.8 ± 1.1	4.8 ± 0.2	10	−65.4 ± 1.5	5.1 ± 0.3	6	−81.6 ± 1.1[a]	4.6 ± 0.1	6			
FGF13U	−51.0 ± 0.5[a]	4.4 ± 0.1[a]	11	−52.0 ± 0.7[a]	4.5 ± 0.1	6	−78.9 ± 0.6[a]	4.6 ± 0.1	7			
FGF13U$^{P/Q}$	−53.1 ± 1.2	4.6 ± 0.1	6	−52.4 ± 1.4[a]	5.0 ± 0.3	5	−73.8 ± 0.9[a]	4.6 ± 0.1	6			

[a] $p < 0.05$ *versus* none. $V_{1/2}$ and k obtained by fitting data to Boltzmann distribution.

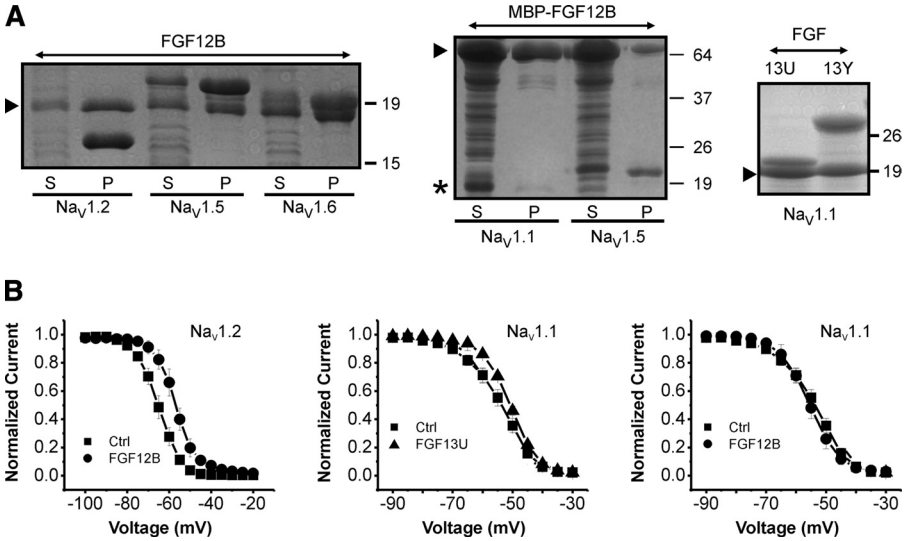

FIGURE 3. **Differential interaction for individual FHF and Na$_V$1 pairs.** *A*, Coomassie-stained gels showing the supernatant of bacterial cell lysate (*S*), or the metal-affinity purified protein (*P*) after co-expression in *E. coli* of the indicated His$_6$-tagged Na$_V$1.x C terminus and the untagged FGF12B (*left*), MBP-tagged 12B and His$_6$-tagged Na$_V$1.1 or Na$_V$1.5 (*middle*), and untagged FGF13U or FGF13Y with His$_6$-tagged Na$_V$1.1 (*right*). The *arrowhead* indicates the FGF12B (*left*), MPB-FGF12B (*middle*) and His$_6$-tagged Na$_V$1.1 (*right*). The * indicates the position of Na$_V$1.1^{CT} in the lysate (*middle*). Position of M$_w$ markers are indicated on the *right*. *B*, steady-state inactivation data for Na$_V$1.1 and Na$_V$1.2 with the indicated FHF or without an added FHF (*Ctrl*). *Symbols* at each test potential show average ± S.E. *Lines* show fits to Boltzmann distributions (see "Experimental Procedures"); parameters, statistics, and *N* are provided in Table 1.

Fig. 2*F*, the GST-tagged Na$_V$1.5^{CT} was efficiently purified by glutathione-agarose and the His$_6$-tagged FGF12B was purified by the Co^{2+}-affinity resin, but neither protein co-purified with its co-expressed partner. Thus, although the intact Na$_V$1.5^{CT} containing amino acids 1773–1908 was sufficient for binding FGF12B, two separate segments each containing a fraction of 1773–1908, but together covered the entire range, were unable to support binding individually.

*Specificity for Interactions between Specific FHFs and Individual Na$_V$1 C Termini*—The utility of our binding assay allowed us also to investigate whether any of the previously reported pairwise specificity for interaction was affected by the distal regions of the Na$_V$1.x^{CT}. We therefore tested, following a similar overall strategy as used for Na$_V$1.5^{CT} in Fig. 2, whether FGF12B bound to Na$_V$1.1, Na$_V$1.2, and Na$_V$1.6. To probe the interaction with Na$_V$1.1^{CT} we employed a slightly different strategy, use of a MBP-tagged FGF12B and His$_6$-tagged Na$_V$1.1 or Na$_V$1.5, because the untagged version of FGF12B migrated at the identical position to the His$_6$-tagged Na$_V$1.1^{CT}, thus precluding our ability to identify the co-purified protein by Coomassie staining. For other FHF-Na$_V$1.x^{CT} pairs, we varied the acrylamide concentration in the gels, used a gradient gel system, or employed a truncated Na$_V$1.x^{CT} construct (if binding was maintained) to achieve separation. We found that, in addition to the Na$_V$1.5^{CT}, FGF12B co-purified with the Na$_V$1.2^{CT} and Na$_V$1.6^{CT}, but not with the Na$_V$1.1^{CT} (Fig. 3*A*). The lack of FGF12B binding to Na$_V$1.1^{CT} was not because of the MBP tag, since the MBP-FGF12B retained its ability to bind to the Na$_V$1.5^{CT}. Nor was it because the Na$_V$1.1^{CT} was incapable of interacting with any FHFs. Fig. 3*A* shows that the His$_6$-tagged Nav1.1^{CT} efficiently pulled down two different FGF13 splice variants.

Because binding between FGF12B and either Na$_V$1.2 or Na$_V$1.6 was not previously observed with the yeast-two hybrid approach (3), we therefore tested our results by determining whether Na$_V$1.2 was functionally modulated by FGF12B. Co-expression of FGF12B with Na$_V$1.2 in HEK cells increased current density (180 ± 27 *versus* 80 ± 4.5 pA/pF for Na$_V$1.2 expressed with the control vector, $p = .01$) and shifted the $V_{1/2}$ for steady-state inactivation from −65.0 ± 1.3 mV to -57.0 ± 1.6 mV ($p = 0.003$) in cells expressing Na$_V$1.2 with the control vector (Fig. 3*B*), consistent with the binding data.

We also tested whether Na$_V$1.1 was modulated by FGF12B or FGF13U, since FGF12B did not bind to the Na$_V$1.1^{CT} in our assay and FGF13U did. We compared whole-cell Na^+ currents from HEK cells stably expressing Na$_V$1.1 to cells additionally transfected with FGF12B or FGF13U. The addition of neither FGF12B nor FGF13U affected current density compared with control cells expressing an empty vector (110 ± 13, 116 ± 13; and 116 ± 23 pA/pF for control, FGF12B, and FGF13U, respectively; $p > 0.05$ *versus* control for each). However, as seen in Fig. 3*B* (and Table 1), FGF13U shifted the $V_{1/2}$ for steady-state inac-

tivation to −51.0 ± 0.5 mV from −54.1 ± 1.5 mV for untransfected controls ($p = .04$); the non-binding FGF12B had no effect ($V_{1/2}$ = −55.1 ± 1.5 after the addition of FGF12B, $p = 0.64$ *versus* control). Thus, functional modulation of a specific FHF isoform on an individual $Na_V1.x$ channel correlates with that FHF isoform ability to bind to the individual $Na_V1.x$ CT in our co-expression assay. Moreover, the interaction between FGF12B and $Na_V1.2^{CT}$, $Na_V1.5^{CT}$, and $Na_V1.6^{CT}$, but not $Na_V1.1^{CT}$ demonstrates specificity for FGF12B binding among specific $Na_V1.x$ C termini.

The Human Single Nucleotide Polymorphism (SNP) P149Q Affects Interaction with $Na_V1.x$ CTs and Abolishes Functional Modulation—We then turned our attention to binding determinants within the FHFs, since they could also contribute to this pairwise specificity. Our attention was drawn to a non-synonymous SNP in human FGF12 (rs17852067), which generates P211Q in FGF12A and P149Q in FGF12B and alters a residue in the core that is conserved among all FHFs (Fig. 4*A*). We tested whether this altered amino acid affected binding and had functional implications. To visualize its location within the core we mapped Pro^{149} in FGF12B to Pro^{154} in FGF13U since the FGF12 crystal structure did not include Pro^{149} (Fig. 4*A*). This shows that Pro^{149} in FGF12B lies on the surface and on a different face from a previously proposed $Na_V1.x$ interaction site on FHFs (9). Nevertheless, mutating Pro^{149} to Gln ($FGF12B^{P/Q}$) affected interaction with Na_V1 C termini. In comparison to wild-type FGF12B, $FGF12B^{P/Q}$ did not bind to the $Na_V1.2^{CT}$ (Fig. 4*B*), suggesting that a single P to Q mutation, distinct and distant from the previously identified (9) $Na_V1.x$ interaction site within FHFs, was able to disrupt interaction with the $Na_V1.2^{CT}$. Binding of $FGF12B^{P/Q}$ to the $Na_V1.5^{CT}$ and the $Na_V1.6^{CT}$ was preserved (Fig. 4*B*), highlighting the specificity of interactions between individual FHFs and distinct $Na_V1.x^{CT}$s observed above. The dominance of this proline was not restricted to FGF12B; mutation of the homologous Pro^{154} to Gln in FGF13U ($FGF13U^{P/Q}$) disrupted the FGF13U-$Na_V1.1$ interaction (Fig. 4*B*; compare Fig. 3*A* for binding of wild-type FGF13U to $Na_V1.1$). In contrast, $Na_V1.2$, $Na_V1.5$, and $Na_V1.6$ bound both wild-type (see supplemental Fig. S1 for binding of wild type FGF13) and $FGF13U^{P/Q}$ (Fig. 4*B*). To test whether mutation of Pro^{154} in FGF13U affected interaction with the entire channel, we expressed a His_6 tag FGF13U or $FGF13U^{P/Q}$ in a cell line stably expressing $Na_V1.1$ and co-immunoprecipitated $Na_V1.1$. As shown in Fig. 4*C*, FGF13U co-immunoprecipitated $Na_V1.1$ but the non-binding $FGF13U^{P/Q}$ did not.

Functional testing of the consequences of these Pro to Gln mutants supported the binding studies and the identification of the Pro residue as a key interaction determinant. As shown previously in Fig. 3*B* and Table 1, co-expression of FGF12B with $Na_V1.2$ shifted the $V_{1/2}$ for steady state inactivation by ~+10 mV. In contrast, co-expression of the non-binding $FGF12B^{P/Q}$ was without effect on steady state inactivation (Fig. 4*D*) and did not alter current density ($p > 0.05$). Co-expression of $FGF12B^{P/Q}$ also did not affect steady-state inactivation of $Na_V1.1$ channels nor current density, consistent with the lack of effect of FGF12B on $Na_V1.1$ function, and that neither wild-type nor $FGF12B^{P/Q}$ bound to the $Na_V1.1^{CT}$. In contrast, co-expression of either FGF12B or $FGF12B^{P/Q}$ shifted the $V_{1/2}$ for $Na_V1.5$ channels, consistent with the observation that both versions bind to the $Na_V1.5^{CT}$ in our assay. The consequence on functional effects of the P/Q mutation in FGF13U also correlated with the binding data. Co-expression of $FGF13U^{P/Q}$, which did not bind $Na_V1.1^{CT}$, did not affect $Na_V1.1$ steady-state inactivation in contrast to wild-type FGF13U (Fig. 4*D* and Table 1). On the other hand, co-expression of FGF13U or $FGF13U^{P/Q}$ shifted the $V_{1/2}$ for $Na_V1.2$ and $Na_V1.5$ steady-state inactivation ~+10 mV (Fig. 4*D* and Table 1), correlating with the positive interactions seen for both FGF13U and $FGF13U^{P/Q}$ with the $Na_V1.2^{CT}$ and $Na_V1.5^{CT}$. Thus, these functional data confirm that binding of a FHF to a $Na_V1.x^{CT}$ in our assay correlates with the ability of that FHF to modulate the $Na_V1.x$ current. Moreover, these data suggest that the SNP in FGF12B could be pathogenic by altering Na^+ channel function.

Affinities for Specific FHFs and Individual $Na_V1.x$ CTs Confirm the Dominance of Pro^{154}—The loss of interaction between $Na_V1.2$ and $FGF12B^{P/Q}$ and the maintenance of interaction between the Pro mutants and the $Na_V1.5$ and $Na_V1.6$ C termini suggested that specific FHFs have different affinities for distinct $Na_V1.x$ C termini. A corollary to this hypothesis is that there are several determinants for interaction between specific FHF isoforms and individual Na_V1 C termini, and that determinants other than the key Pro residue are sufficient to maintain interaction. We tested this assumption by measuring quantitative binding affinities between specific FHFs and individual $Na_V1.x$ C termini using surface plasmon resonance (SPR, Biacore). FGF12B, $FGF12B^{P/Q}$, or FGF13U were immobilized on a biosensor chip and increasing concentrations of $Na_V1.1^{CT}$, $Na_V1.2^{CT}$, and $Na_V1.5^{CT}$ were flowed over the chip. Fig. 5 and Table 2 show that binding between FGF12B and the $Na_V1.1^{CT}$ was weak compared with the $Na_V1.2^{CT}$ or $Na_V1.5^{CT}$, thereby explaining the lack of interaction observed in our co-purification assays and providing a minimum for the affinity required for interaction in that assay. The P/Q mutation in FGF12B abolished binding for the $Na_V1.2^{CT}$. Consistent with the co-purification experiments in Fig. 4, however, the P/Q mutant had minimal effect upon interaction of FGF12B with the $Na_V1.5^{CT}$. For the $Na_V1.1^{CT}$ and the $Na_V1.2^{CT}$, FGF13U bound more avidly than FGF12B. Thus, the overall pattern observed with the SPR data were consistent with that observed in the qualitative co-purification and the electrophysiological assays. Moreover, the quantitative SPR data provide a rank order of affinities for both the FHFs and for the Na_V1^{CT} domains: FGF13U > FGF12B > $FGF12B^{P/Q}$; and $Na_V1.5^{CT} > Na_V1.2^{CT} > Na_V1.1^{CT}$.

Disruption of Interaction between a FHF and a $Na_V1.x$ CT Affects FHF Localization to the Axon Initial Segment in Hippocampal Neurons—The SCA27 mutation F145S in FGF14 disrupts interaction with $Na_V1.2$ and prevents efficient targeting of FGF14 to the AIS (5), where Na^+ channels are concentrated. We thus tested whether the $FGF12B^{P/Q}$ mutant, which similarly fails to interact with $Na_V1.2$, would affect the targeting of FGF12B to the AIS in hippocampal neurons. GFP-tagged FGF12B or $FGF12B^{P/Q}$ was transfected into cultured rat hippocampal neurons and the AIS was identified by staining for ankyrin G. The presence or absence of the GFP-tagged FGF12B or $FGF12B^{P/Q}$ in the AIS was then scored by an observer blinded to the identity of which FGF12B was transfected (Fig.

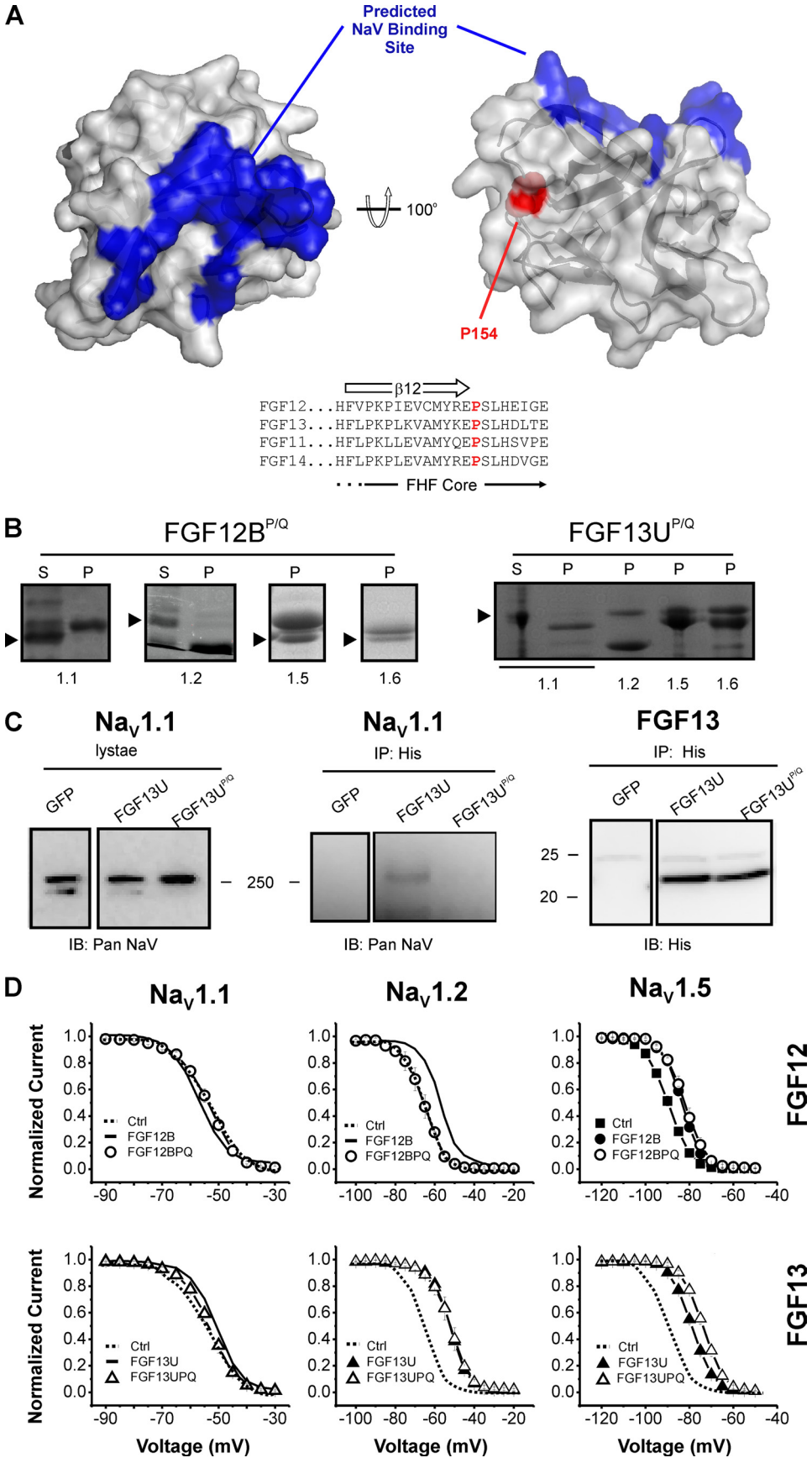
A
Predicted
NaV Binding
Site
100°
P154
β12
FGF12...HFVPKPIEVCMYREPSLHEIGE
FGF13...HFLPKPLKVAMYKEPSLHDLTE
FGF11...HFLPKLLEVAMYQEPSLHSVPE
FGF14...HFLPKPLEVAMYREPSLHDVGE
FHF Core
B
FGF12B P/Q
FGF13U P/Q
S P S P P P
S P P P P
1.1 1.2 1.5 1.6
1.1 1.2 1.5 1.6
C
NaV1.1
lystae
NaV1.1
IP: His
FGF13
IP: His
GFP FGF13U FGF13U P/Q
250
25
20
IB: Pan NaV
IB: Pan NaV
IB: His
D
NaV1.1
NaV1.2
NaV1.5
Normalized Current
Ctrl
FGF12B
FGF12BPQ
FGF12
Ctrl
FGF13U
FGF13UPQ
FGF13
Voltage (mV)
Voltage (mV)
Voltage (mV)

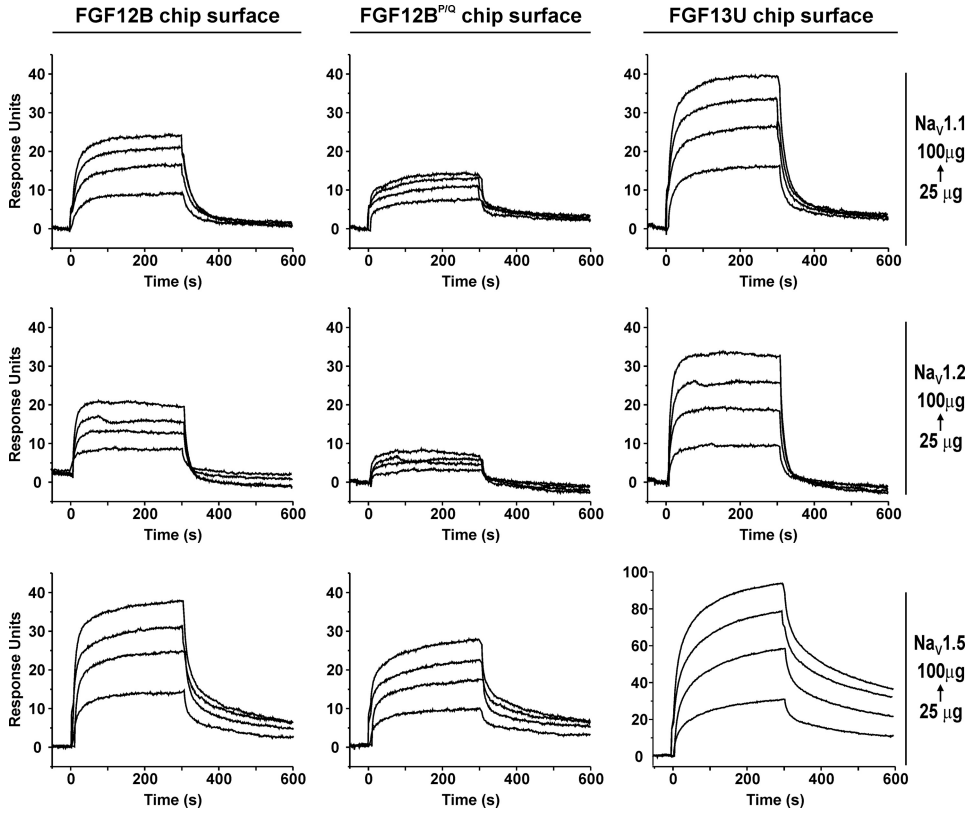

FIGURE 5. **Individual FHF and Na$_V$1.x pairs show specific affinities for interaction that are affected by the P/Q mutation.** Typical surface plasmon resonance (Biacore) sensorgrams for the indicated FHF/Na$_V$1.x pairs. Fitting parameters are shown in Table 2.

TABLE 2

Binding constants and K_d for the indicated Na$_V$1.x channel / FHF pair

	FGF12B			FGF12B$^{P/Q}$			FGF13U		
	k_{on}	k_{off}	K_d	k_{on}	k_{off}	K_d	k_{on}	k_{off}	K_d
	ms^{-1}	s^{-1}	μM	ms^{-1}	s^{-1}	μM	ms^{-1}	s^{-1}	μM
Na$_V$1.1	150	0.056	380	-	-	-	4,900	0.034	7.0
Na$_V$1.2	2,400	0.110	46	-	-	-	3,400	0.057	17
Na$_V$1.5	7,490	0.004	0.6	4,500	0.003	0.7	4,100	0.002	0.5

6). In 20 of 38 neurons GFP-tagged FGF12B was observed in the AIS; GFP-tagged FGF12B$^{P/Q}$ was observed in the AIS in 12 of 43 neurons, $\chi^2 = 4.99$, $p = 0.001$. Thus, similar to the SCA27 mutation in FGF14 that blocks interaction with Na$_V$1.2 and affects targeting of FGF14 to the AIS (5), the P149Q mutation in FGF12B decreases efficient interaction with Na$_V$1.2 (Fig. 4*B*), and affects targeting of FGF12B to the AIS.

DISCUSSION

FHFs belong to a growing list of proteins such as calmodulin (13, 14, 16) and Na^+ channel β subunits (17) that serve as binding partners for the Na$_V$1.x CTs and can modulate Na^+ channel function. Nevertheless, the manner by which FHFs interact with Na^+ channels and thereby impart modulation has remained obscure. The interaction site originally identified on Na$_V$1.9, in the proximal portion of the channel C terminus (2, 3), is conserved among most VGSCs, yet FGF12B was initially shown not to bind to the C terminus of any other VGSC except Na$_V$1.5. Moreover, functional analysis of individual FHF-Na$_V$1.x pairs showed specificity of modulation, even though all 4 FHFs share homology within the proposed face for Na$_V$1.x interaction. The molecular mechanisms responsible for these stereotypic interactions have not been elucidated.

Using a method of co-purification of recombinant proteins co-expressed in bacteria, with which we have successfully established interactions among ion channels and their intracellular binding partners (12, 13, 18–21), and validated by electro-

FIGURE 4. **The P149Q (FGF12B) and P154Q (FGF13U) affect interaction with certain Na$_V$1.x C termini and modulation of the respective Na$_V$1.x channel.** *A*, surface of FGF13 (PDB: 3HBW). Highlighted in *blue* are the 8 amino acids that comprise the predicted Na$_V$1.x binding site (9); in *red* is P154 (using FGF13U numbering, homologous to Pro^{149} in FGF12B). *B*, Coomassie-stained gel showing bacterial cell supernatant (*S*) or metal affinity purified material (*P*) for the indicated combinations of a His$_6$-tagged Na$_V$1.x with the indicated mutant FHF. The FHF position is indicated by an *arrowhead*. *C*, immunoblots with the indicated antibodies (*IB*) of whole cell lysates or after immunoprecipitation with the indicated antibodies (*IP*) showing that Na$_V$1.1 co-immunoprecipitates with FGF13U, but not the mutant FGF13U$^{P/Q}$. *D*, intermediate inactivation for the indicated Na$_V$1.x/FHF pairs. Protocol and details are the same as in Fig. 1*E* and Fig. 3*D*. Note that data previously shown in Fig. 1*E* and Fig. 3*D* are displayed as a *solid* or *dashed line*, without symbols. Fit parameters, statistics, and *N* are in Table 1.

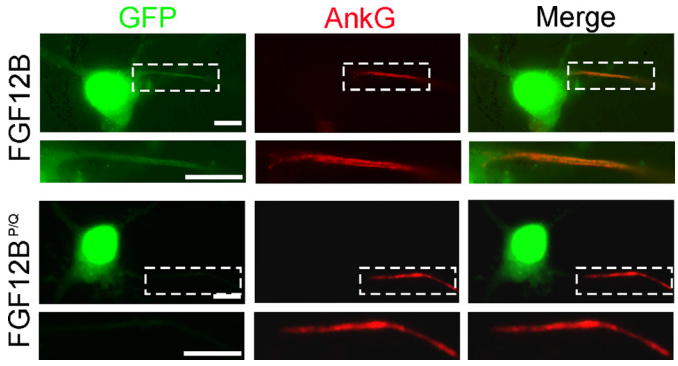

FIGURE 6. **The P149Q mutation affects targeting of FGF12B to the axon initial segment in cultured hippocampal neurons.** Representative epifluorescence images of hippocampal neurons transfected with WT or P149Q mutated FGF12B tagged with GFP at the C terminus and processed for immunocytochemistry for AnkG (*red*) to identify the AIS (in *box*). *Left*, GFP; *middle*, AnkG; and *right*, merged. Scale bar, 10 μm.

physiological recordings for key pairs, we established that interactions between individual FHFs and specific Na$_V$1.x CTs are more wide-spread than previously reported. For example, among the new pairings we observed are FGF12B and FGF13U with Na$_V$1.2. Still, some interesting specificity remains, because we established that FGF12B cannot bind the Na$_V$1.1 CT or modulate Na$_V$1.1 function.

The origin of this specificity remains unclear, but we were able to provide new information about the binding sites within both the Na$_V$1.x CTs and the FHFs. Most importantly, we established new and essential determinants within the Na$_V$1.x CTs. Although the minimal binding site for FGF12B within the Na$_V$1.5 CT was previously mapped to the most proximal 60 amino acids (3), our data suggested an additional requirement of at least another 60 amino acids. The reason(s) for this discrepancy is not clear, but may be due to the use of a sensitive, but not specific, yeast two-hybrid strategy that utilizes an indirect assessment of interaction to perform the pervious mapping experiments (3). In contrast, we used a binding assay that entails co-purification of purified recombinant proteins, allowing us to confirm a direct and stoichiometric interaction between FGF12B and the specific Na$_V$1.5 CT domain tested. Our approach allowed us to demonstrate several new pairwise interactions. We found that FGF12B can bind to the Na$_V$1.6 and Na$_V$1.2 C termini. Further, this approach allowed us to rule out the contribution of any other factor or protein modification not yet identified since we were able to observe a direct interaction. Finally, we confirmed our results obtained with recombinant protein domains through co-immunoprecipitation experiments that employed the intact channel and through electrophysiological testing. Interestingly, although the Na$_V$1.5^{CT} construct containing amino acids 1773–1887 was unable to bind FGF12B while 1773–1908 was able, we could not identify a binding site between amino acids 1887–1908. Thus the most parsimonious explanation is that determinants in both the proximal and more distal regions of the Na$_V$1.5 C terminus are required.

We were also able to provide new information about the binding site on FHFs for VGSC C termini. The initial report suggested that the binding site was within the first third of the FHF core domain (2) while some subsequent studies pointed to contributions from the alternatively spliced FHF N-terminal extensions. Comparison of the effects of individual FHFs on specific Na$_V$1.x currents also suggested isoform-specific interactions and modulation (7, 8). A more recent study proposed that the interaction site comprises one face of the FGF-like core formed by of a set of 8 amino acids scattered throughout the core primary sequence (9). Our mapping studies also highlight a key region, not previously identified, within the FHFs that is important for interaction and for Na^+ channel modulation. Specifically, within the FHF core we demonstrated that mutation of a single Pro (conserved in all FHFs) can abolish interaction of certain FHFs with some individual Na$_V$1.x C termini (but not others), can reduce the affinity of interaction with Na$_V$1.x CTs, and can alter targeting of FGF12B to the AIS of hippocampal neurons. This Pro (Pro^{149} in FGF12B; Pro^{154} in FGF13U) lies on a face of the FHF core remote from the binding surface recently predicted (9). As interactions with Na$_V$1.5 (but not Na$_V$1.1) were preserved with the FGF13 P154Q mutant, these data together suggest that Na$_V$1.5 interacts differently with FHFs compared with Na$_V$1.1 and thus provide further evidence for pair-specific interactions. In combination with previous data demonstrating the role of the remote FHF face, our data suggest that there are multiple interaction sites within the FHFs, each of which might contribute to the pairwise-specificity. This hypothesis fits well with our finding that multiple, and distinct regions of the Na$_V$1.5^{CT} appear necessary for FGF12B interaction.

It is notable that the recent crystal structure of the FGF13 core demonstrates that the key Pro is at the end of the conserved FGF-like core domain and, although distant in the primary sequence, it is nearly adjacent in the folded protein to the most N-terminal amino acid of the core (E10 of FGF13U in PDB: 3HBW), where the alternatively spliced N terminus would insert. This suggests two independent, but not mutually exclusive, hypotheses that could help explain how specific FHF splice variants have different effects upon individual Na$_V$1.x channels. First, the most distal region of the variable N terminus could contribute to the binding site on FHFs, providing further specificity to the interaction between specific FHFs and individual Na$_V$1.x pairs. Second, the binding site on the FHF may not include the variable N terminus, but its proximity to the binding site (which includes the key Pro) may allow the variable N terminus to interact with other domains of the channel and thereby influence channel modulation in a variant-specific manner. No clinical data regarding the FGF12B polymorphism (rs17852067) have been reported, so its relevance for physiology or pathophysiology is not clear. Nevertheless, the variant proved informative for helping map key determinants for interaction with Na$_V$1.x CTs.

Acknowledgments—We thank Theodore Cummins (Indiana University) for the gift of the expression construct for Na$_V$1.2, Nenad Bursac (Duke University) for the expression construct for Na$_V$1.5, Al George (Vanderbilt) for the cell line stably expressing Na$_V$1.1, and Van Bennett (Duke University) for the ankyrin G antibody.

REFERENCES

1. Goldfarb, M. (2005) *Cytokine Growth Factor Rev.* **16,** 215–220
2. Liu, C. J., Dib-Hajj, S. D., and Waxman, S. G. (2001) *J. Biol. Chem.* **276,** 18925–18933
3. Liu, C. J., Dib-Hajj, S. D., Renganathan, M., Cummins, T. R., and Waxman, S. G. (2003) *J. Biol. Chem.* **278,** 1029–1036
4. van Swieten, J. C., Brusse, E., de Graaf, B. M., Krieger, E., van de Graaf, R., de Koning, I., Maat-Kievit, A., Leegwater, P., Dooijes, D., Oostra, B. A., and Heutink, P. (2003) *Am. J. Hum. Genet.* **72,** 191–199
5. Laezza, F., Gerber, B. R., Lou, J. Y., Kozel, M. A., Hartman, H., Craig, A. M., Ornitz, D. M., and Nerbonne, J. M. (2007) *J. Neurosci.* **27,** 12033–12044
6. Wittmack, E. K., Rush, A. M., Craner, M. J., Goldfarb, M., Waxman, S. G., and Dib-Hajj, S. D. (2004) *J. Neurosci.* **24,** 6765–6775
7. Lou, J. Y., Laezza, F., Gerber, B. R., Xiao, M., Yamada, K. A., Hartmann, H., Craig, A. M., Nerbonne, J. M., and Ornitz, D. M. (2005) *J. Physiol.* **569,** 179–193
8. Laezza, F., Lampert, A., Kozel, M. A., Gerber, B. R., Rush, A. M., Nerbonne, J. M., Waxman, S. G., Dib-Hajj, S. D., and Ornitz, D. M. (2009) *Mol. Cell Neurosci.* **42,** 90–101
9. Goetz, R., Dover, K., Laezza, F., Shtraizent, N., Huang, X., Tchetchik, D., Eliseenkova, A. V., Xu, C. F., Neubert, T. A., Ornitz, D. M., Goldfarb, M., and Mohammadi, M. (2009) *J. Biol. Chem.* **284,** 17883–17896
10. Miloushev, V. Z., Levine, J. A., Arbing, M. A., Hunt, J. F., Pitt, G. S., and Palmer, A. G., 3rd. (2009) *J. Biol. Chem.* **284,** 6446–6454
11. Chagot, B., Potet, F., Balser, J. R., and Chazin, W. J. (2009) *J. Biol. Chem.* **284,** 6436–6445
12. Wang, C., Wang, H. G., Xie, H., and Pitt, G. S. (2008) *J. Neurosci.* **28,** 1865–1870
13. Kim, J., Ghosh, S., Liu, H., Tateyama, M., Kass, R. S., and Pitt, G. S. (2004) *J. Biol. Chem.* **279,** 45004–45012
14. Tan, H. L., Kupershmidt, S., Zhang, R., Stepanovic, S., Roden, D. M., Wilde, A. A., Anderson, M. E., and Balser, J. R. (2002) *Nature* **415,** 442–447
15. Cormier, J. W., Rivolta, I., Tateyama, M., Yang, A. S., and Kass, R. S. (2002) *J. Biol. Chem.* **277,** 9233–9241
16. Mori, M., Konno, T., Ozawa, T., Murata, M., Imoto, K., and Nagayama, K. (2000) *Biochemistry* **39,** 1316–1323
17. Rusconi, R., Scalmani, P., Cassulini, R. R., Giunti, G., Gambardella, A., Franceschetti, S., Annesi, G., Wanke, E., and Mantegazza, M. (2007) *J. Neurosci.* **27,** 11037–11046
18. Kim, J., Ghosh, S., Nunziato, D. A., and Pitt, G. S. (2004) *Neuron* **41,** 745–754
19. Maltez, J. M., Nunziato, D. A., Kim, J., and Pitt, G. S. (2005) *Nat. Struct. Mol. Biol.* **12,** 372–377
20. Ghosh, S., Nunziato, D. A., and Pitt, G. S. (2006) *Circ. Res.* **98,** 1048–1054
21. Thomsen, M. B., Wang, C., Ozgen, N., Wang, H. G., Rosen, M. R., and Pitt, G. S. (2009) *Circ. Res.* **104,** 1382–1389